

Kinetics and Thermodynamic Study on the Oxidation of 1,1-Dimethylhydrazine by Iodine: A MNDO and DFT Approach

**David Ebuka ARTHUR^{*}, Adamu UZAIRU,
Philip John AMEJI and Israel Emmanuel EDACHE**

Department of Chemistry, Ahmadu Bello University Zaria, Nigeria

(* Corresponding author's e-mail: hanslibs@myway.com)

Received: 28 August 2014, Revised: 5 January 2015, Accepted: 17 February 2015

Abstract:

The reaction mechanism of the oxidation of 1,1-dimethylhydrazine by iodine was examined using semi-empirical and density functional theory methods. The oxidation proceeded via an independent pathway which was monitored and the results of the kinetic and thermodynamic study were determined. It was found that the reactant as seen by their determined binding energy would readily undergo a two-step reaction leading to the decomposition of the reactants and the formation of more stable products.

Keywords: 1,1-dimethylhydrazine, DFT, MNDO, Iodine, oxidation reaction

Introduction

1,1-dimethylhydrazine is employed as a high-energy fuel for thrusters and small electrical power generating units. It is also used in chemical synthesis for manufacturing plant growth regulators, as a stabilizer for fuel additives in photographic chemicals and as an absorbent for acid gases [1-3].

Research has shown that individuals may be exposed to 1,1-dimethylhydrazine in the work place, in the ambient atmosphere from its use as rocket fuel and from spills, leaks, venting during loading transfer and storage. In the atmosphere, 1,1-dimethylhydrazine undergoes ozonolysis and also reacts with hydroxyl radicals to produce 1,1-dimethylnitrosamine which is a potent carcinogen as reported in [1,4].

Personal exposure to 1,1-dimethylhydrazine can be measured in the blood, urine and tissues of exposed persons [5]. Acute inhalation or exposure of humans to 1,1-dimethylhydrazine has been observed to result in nose and throat irritation, mold conjunctivitis, nausea and vomiting [6]. It is highly corrosive and irritating to the skin, eyes, mucous membranes and neurological symptoms were observed in a man burned by 1,1-dimethylhydrazine [8]. Central nervous system (CNS) stimulation and convulsions have been reported in animals acutely exposed to 1,1-dimethylhydrazine by ingestion [9]. Liver damage in humans may occur from chronic (long term) exposure to 1,1-dimethylhydrazine [10]. Hemolytic anemia and CNS effects such as convulsive seizures, have been observed in animals chronically exposed to 1,1-dimethylhydrazine via inhalation [11].

Iodine, on the other hand is an essential component of human diet and it appears to be the heaviest required element in a diet (the thyroid gland needs iodine to make hormones). The human body requires iodine for some complex chemical reactions in the body but cannot make it. Hence, iodine comes from food, although biochemical literature serves that as a rule there is little iodine in food, unless added during processing which is now the case with salt.

Iodine is also used for treating skin diseases caused by fungus (cutaneous sporotrichosis), treating fibrocystic breast disease, preventing breast cancer, eye disease, diabetes, heart diseases and stroke, as an expectorant. These and many other reasons make the study of iodine interesting. Iodine was reported to oxidize quantitatively most substances containing the -NH-NH- group [12]. This reaction is the basis for

one of the standard analytical procedures to titrate hydrazine and related substances, such as isonicotinoylhydrazine and hydrazonebenzene, which are widely used in the pharmaceutical industry because of their bacteriostatic properties. The mechanism of oxidation of hydrazine and its derivatives by iodine has been the subject of several studies, but among which no complete agreement was found.

Molecular orbital calculations have been examined for complicated reaction systems that are difficult to study experimentally. However, no calculation has been done with 1,1-methylhydrazine and its derivatives, probably due to the complication of these species. Computational chemistry methods can be used to explore the theoretical chemistry behind reactive systems, to compare chemical reactivity of different systems and by extension to predict the reactivity or plausible reaction pathways of new systems [13]. Semi-empirical models AM1, PM3, and MNDO are often used in computational chemistry because they allow the study of systems that are out of reach of the more accurate methods. These models have also been found to be very effective for systems that contain elements beyond 4th row in the periodic table.

In theoretical studies when subjecting compounds of interest to *ab initio* or density functional theory (DFT) methods, choices of a theoretical method and a basis set are very imperative in obtaining reliable results. Unfortunately, the basis sets required for elements beyond the 4th row in the periodic table are somewhat limited, although various accurate theoretical methods such as B3LYP have been currently developed. Theoretical studies on compounds containing iodine, a 5th period halogen atom have been found to be more scarce compared to those containing F, Cl, or Br. Heavy elements like iodine have a large number of inner shell electrons which are in general less important for the chemical reactivity and bonding modes. However, the needs for a large number of basis sets or functions to describe the corresponding orbitals cannot be over emphasized. This makes computations with heavy elements like iodine expensive and very time consuming. In addition, compounds containing iodine atom have been found to be of important in many chemical reactions especially in fringe science.

In the present paper we report the results of computational studies on the mechanism of the oxidation of 1,1-dimethylhydrazine, a derivative of hydrazine, by iodine. In this study, the reacting species were first optimized using MM (molecular mechanics), then finally by MNDO (a semi-empirical method which neglects differential overlap of electron orbitals) and DFT (density functional theory). For the density functional theory studies, geometry optimizations of all compounds and transition states were carried out at 6311 + G** basis set which adds polarization functions to hydrogens of the 6-311G* basis set. Available for elements H - Ca, Ga - Kr and I, by using the B3LYP approximation method for better results.

Computational methods

The Spartan 14 v1.1.0 Molecular Mechanics method, semi-empirical (MNDO) and DFT methods were used on a Microsoft Windows 8 operating system, with Intel® Core i3 CPU, 4.00GB of RAM.


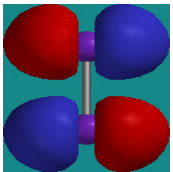
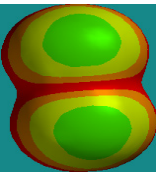
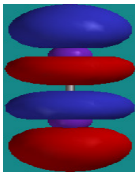
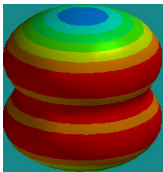
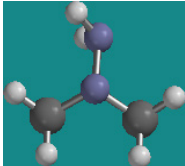
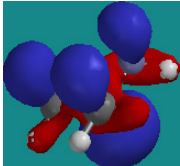
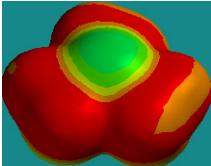
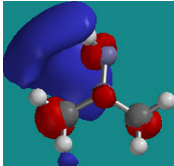
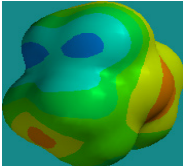
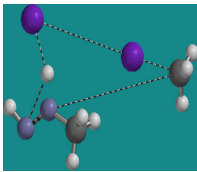
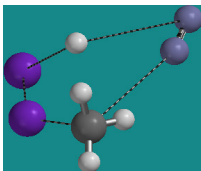
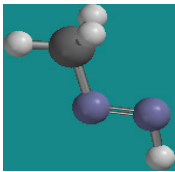
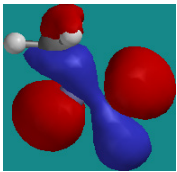
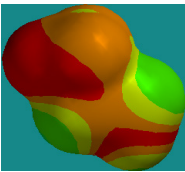
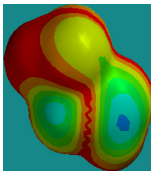
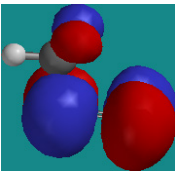
The starting geometries for the semi-empirical and DFT calculation were first optimized and calculated using the MM method to remove strain energy. The MM optimized species were then used for the respective MNDO and DFT calculations [14]. Geometry optimizations of all compounds and transition states were carried out using a 6311+G** basis set with a B3LYP functional.


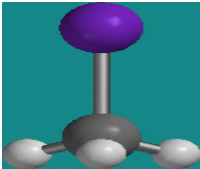
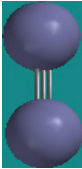
The optimized geometries of the transition states and products were confirmed in terms of vibrational analysis [9]. The transition state for each step was located and confirmed by animating the vibration corresponding to the reaction coordinate by selecting the imaginary frequency at the top of the list of frequencies on the IR tab.

Results and discussion

The computational studies of the activation energies determined suggest the reaction cannot proceed without the inclusion of a catalyst to the reaction media [15]. This deduction is due to the positive value of the activation energy for the second transition state when the computation is done using the DFT method. The dissociation or energy gap determined agrees with the preferred state suggested by the literature pertaining to the product, this was found when comparing the energy gap of the products with that of the reacting species.

Table 1 Picture of the Frontier orbitals and the 3D structure of the species.

		HOMO and electron density surface for HOMO		LUMO and electron density surface for LUMO	
I ₂					
(CH ₃) ₂ N-NH ₂					
TS1					
TS2					
Intermediate					

	HOMO and electron density surface for HOMO	LUMO and electron density surface for LUMO
HI		
CH ₃ I		
N ₂		

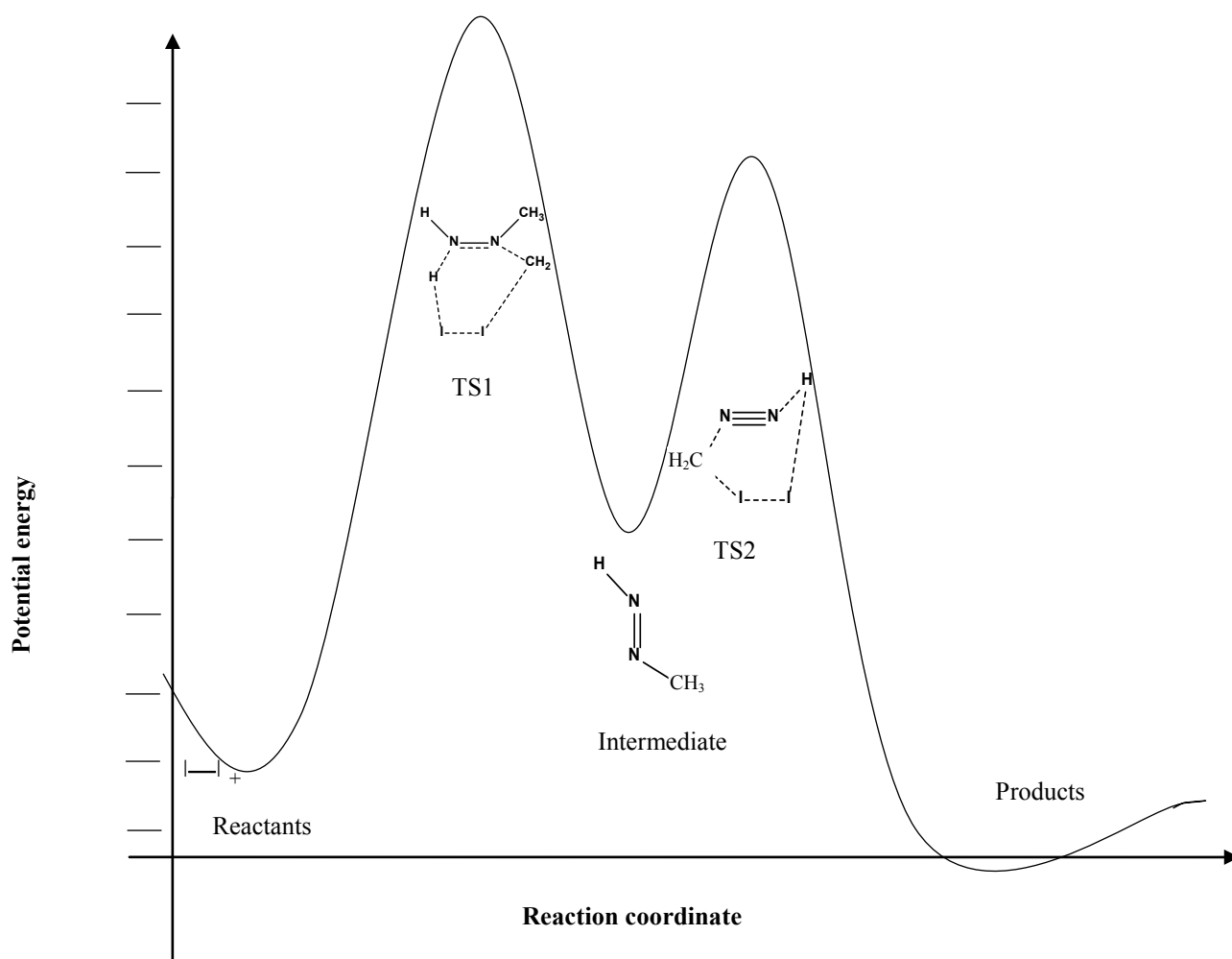


Figure 1 A sketch of the reaction coordinate profile for the reaction of 1,1-dimethylhydrazine with iodine using DFT computational tools.

Table 2 Bond length and bond angle of 1,1-dimethylhydrazine determined using MNDO.

Bond length	(Å)	Bond angle	(°)
C(4)-H(12)	1.124	H(12)-C(4)-H(11)	108.718
C(4)-H(11)	1.121	H(12)-C(4)-H(10)	108.431
C(4)-H(10)	1.120	H(12)-C(4)-N(2)	112.608
C(3)-H(9)	1.123	H(11)-C(4)-H(10)	108.535
C(3)-H(8)	1.121	H(11)-C(4)-N(2)	109.140
C(3)-H(7)	1.121	H(10)-C(4)-N(2)	109.327
N(1)-H(6)	1.013	H(9)-C(3)-H(8)	108.817
N(1)-H(5)	1.011	H(9)-C(3)-H(7)	108.753
N(2)-C(4)	1.466	H(9)-C(3)-N(2)	112.535
N(2)-C(3)	1.466	H(8)-C(3)-H(7)	109.469
N(1)-N(2)	1.378	H(8)-C(3)-N(2)	108.161
		H(7)-C(3)-N(2)	109.071
		C(4)-N(2)-C(3)	114.104
		C(4)-N(2)-N(1)	112.909
		C(3)-N(2)-N(1)	109.337
		H(6)-N(1)-H(5)	111.775
		H(6)-N(1)-N(2)	112.035
		H(5)-N(1)-N(2)	109.373

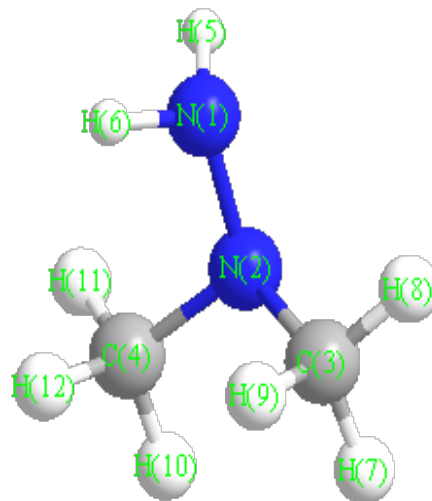


Table 3 Bond length of iodine molecule determined using MNDO.

Bond length	(Å)
I(1)-I(2)	2.736



Table 4 Bond length and bond angles of the Intermediate (methylhydrazine) determined using MNDO.

Bond length	(Å)	Bond angle	(°)
C(3)-H(7)	1.080	H(7)-C(3)-H(6)	110.771
C(3)-H(6)	1.082	H(7)-C(3)-H(5)	110.894
C(3)-H(5)	1.082	H(7)-C(3)-N(1)	110.967
N(2)-H(4)	1.022	H(6)-C(3)-H(5)	108.473
N(1)-C(3)	1.482	H(6)-C(3)-N(1)	107.768
N(1)-N(2)	1.236	H(5)-C(3)-N(1)	107.847
		H(4)-N(2)-N(1)	109.094
		C(3)-N(1)-N(2)	113.426

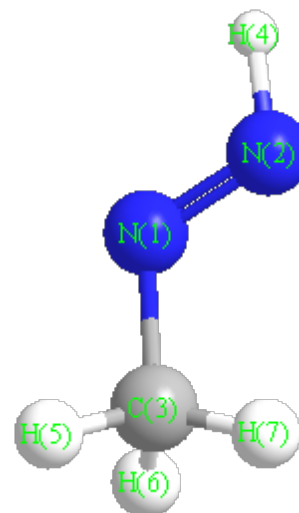


Table 5 Bond length and bond angle of methyl iodide determined using MNDO.

Bond length	(Å)	Bond angle	(°)
C(1)-H(5)	1.085	H(5)-C(1)-H(4)	111.284
C(1)-H(4)	1.085	H(5)-C(1)-H(3)	111.309
C(1)-H(3)	1.085	H(5)-C(1)-I(2)	107.576
C(1)-I(2)	2.182	H(4)-C(1)-H(3)	111.300
		H(4)-C(1)-I(2)	107.575
		H(3)-C(1)-I(2)	107.578

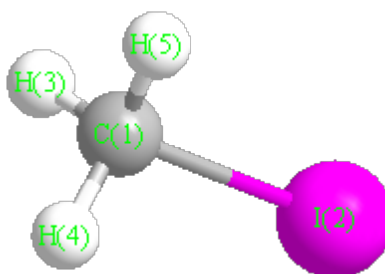


Table 6 Bond length of hydrogen iodide determined using MNDO.

Bond length	(Å)
H(1)-I(2)	1.634

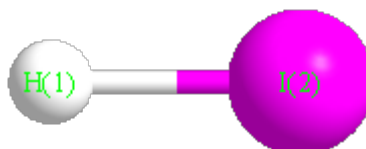
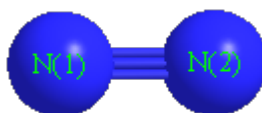


Table 7 Bond length of nitrogen molecule determined using MNDO.

Bond length	(Å)
N(1)-N(2)	1.096



As shown in **Tables 2** and **7**, the bond length of the nitrogen-nitrogen bond decreased from 1.378 Å of 1,1-dimethylhydrazine to 1.096 Å of N₂, other reduced bond lengths suggest an increase in the attractive force between bonded atoms and hence higher stability.

The vibrational modes for the transition states were determined to confirm their respective states, (TS1) i.e. transition state 1 was found to have three imaginary frequencies, while TS2 had just 2.

Table 8 Thermodynamic parameters determined using-semi empirical method (MNDO).

Chemical species	Heat of formation (ΔH°) KJ/mol	Free Gibbs energy (ΔG°) KJ/mol	Entropy (ΔS°) J/mol
I ₂	93.69	35.49	259.34
C ₂ H ₈ N ₂	60.41	305.92	298.65
TS1	549.22	715.93	483.63
CH ₄ N ₂	94.95	202.31	272.29
TS2	412.63	436.83	453.37
HI	92.19	56.64	206.18
CH ₃ I	11.91	54.33	252.29
N ₂	37.06	2.58	191.54

Table 9 Atomic and thermodynamic parameters determined using DFT (B3LYP/6311+G**).

Chemical species	Electronic energy (E) au	Free Gibbs energy (ΔG°) au	Entropy (ΔS°) J/mol
I ₂	-13839.0598	-13839.0851	260.55
C ₂ H ₈ N ₂	-190.5484	-190.4669	294.72
TS1	-14029.6845	-14029.5224	409.54
CH ₄ N ₂	-150.0148	-149.9733	258.11
TS2	-13989.0674	-13988.9567	399.80
HI	-6920.1260	-6920.1388	206.59
CH ₃ I	-6959.4514	-6959.4366	254.30
N ₂	-109.5587	-109.5725	191.42

Table 10 Atomic parameters determined using density functional theory method (B3LYP/6311+G**).

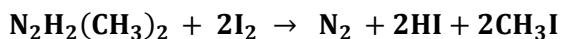
Chemical species	Energy of HOMO (eV) = E-HOMO	Energy of LUMO (eV) = E-LUMO	Binding energy (eV) = E-LUMO – E-HOMO
I ₂	-7.25	-4.16	3.09
C ₂ H ₈ N ₂	-6.26	-0.01	6.25
TS1	-5.97	-3.69	2.28
CH ₄ N ₂	-6.61	-1.76	4.85
TS2	-6.41	-5.26	1.15
HI	-7.71	-1.21	6.50
CH ₃ I	-7.10	-1.36	5.74
N ₂	-12.00	-1.03	10.97

Table 11 Predicted imaginary IR frequency of the suggested transition states using DFT.

Vibrational modes for the transition states	Frequency	Intensity
Transition state 1(TS1)	i82	1.30
	i37	0.27
	i7	0.71
Transition state 2 (TS2)	i625	65.16
	i83	1.91

Thermodynamic parameters

These parameters were determined using the overall equation of the reaction from our proposed mechanism. DFT method was used in calculating the standard entropy, electronic energy and free Gibbs energy of reaction, while the semi-empirical method (MNDO) was used to determine the standard heat of reaction.



1. Standard free Gibbs energy of the reaction ($\Delta G^\circ_{\text{rxn}}$)

$$\begin{aligned} \Delta G^\circ_{\text{rxn}}(298.15\text{K}) &= [\nu_{\text{N}_2} G^\circ_{\text{N}_2} + \nu_{\text{HI}} G^\circ_{\text{HI}} + \nu_{\text{CH}_3\text{I}} G^\circ_{\text{CH}_3\text{I}}] \\ &- [\nu_{\text{N}_2\text{H}_2(\text{CH}_3)_2} G^\circ_{\text{N}_2\text{H}_2(\text{CH}_3)_2} + \nu_{\text{I}_2} G^\circ_{\text{I}_2}] \end{aligned}$$

2. Standard heat of reaction ($\Delta H_{\text{rxn}}^{\circ}$)

$$\Delta H_{\text{rxn}}^{\circ}(298.15\text{K}) = [v_{\text{N}_2} H_{\text{N}_2}^{\circ} + v_{\text{HI}} H_{\text{HI}}^{\circ} + v_{\text{CH}_3\text{I}} H_{\text{CH}_3\text{I}}^{\circ}] - [v_{\text{N}_2\text{H}_2(\text{CH}_3)_2} H_{\text{N}_2\text{H}_2(\text{CH}_3)_2}^{\circ} + v_{\text{I}_2} H_{\text{I}_2}^{\circ}]$$

3. Standard entropy of reaction ($\Delta S_{\text{rxn}}^{\circ}$)

$$\Delta S_{\text{rxn}}^{\circ}(298.15\text{K}) = [v_{\text{N}_2} S_{\text{N}_2}^{\circ} + v_{\text{HI}} S_{\text{HI}}^{\circ} + v_{\text{CH}_3\text{I}} S_{\text{CH}_3\text{I}}^{\circ}] - [v_{\text{N}_2\text{H}_2(\text{CH}_3)_2} S_{\text{N}_2\text{H}_2(\text{CH}_3)_2}^{\circ} + v_{\text{I}_2} S_{\text{I}_2}^{\circ}]$$

4. Energy of reaction

$$\Delta E_{\text{rxn}}^{\circ}(298.15\text{K}) = [v_{\text{N}_2} E_{\text{N}_2}^{\circ} + v_{\text{HI}} E_{\text{HI}}^{\circ} + v_{\text{CH}_3\text{I}} E_{\text{CH}_3\text{I}}^{\circ}] - [v_{\text{N}_2\text{H}_2(\text{CH}_3)_2} E_{\text{N}_2\text{H}_2(\text{CH}_3)_2}^{\circ} + v_{\text{I}_2} E_{\text{I}_2}^{\circ}]$$

Thermodynamic parameters	
$\Delta G_{\text{rxn}}^{\circ}(298.15\text{K})$	-226.32 kJmol ⁻¹
$\Delta H_{\text{rxn}}^{\circ}(298.15\text{K})$	-2.53 kJmol ⁻¹
$\Delta S_{\text{rxn}}^{\circ}(298.15\text{K})$	0.30 kJmol ⁻¹
$\Delta E_{\text{rxn}}^{\circ}(298.15\text{K})$	6140.78 kJmol ⁻¹

Kinetic parameters

The kinetic parameters were determined with the DFT optimized molecules including the activation energy (ΔE_1^{\ddagger} and ΔE_2^{\ddagger}), equilibrium constant (K), Arrhenius factor (A), free Gibbs energy of activation (ΔG_1^{\ddagger} , ΔG_2^{\ddagger}) and rate constants for the steps (k_1 and k_2).

I. Activation energies

$$\Delta E_1^{\ddagger} = E_{\text{Transition State1}} - (E_{\text{N}_2\text{H}_2(\text{CH}_3)_2} + E_{\text{I}_2})$$

and

$$\Delta E_2^{\ddagger} = E_{\text{Transition State2}} - (E_{\text{N}_2\text{CH}_4} + E_{\text{I}_2})$$

II. Equilibrium constant K_{eq}

$$K_{\text{eq}} = \exp\left(\frac{-\Delta G_{\text{rxn}}}{RT}\right)$$

At room temperature (298.15K) and for ΔG_{rxn} in au, this is given by

$$K_{\text{eq}} = \exp(-1060\Delta G_{\text{rxn}})$$

- III. **Reaction rate constants**, k_{rxn} or (k_1 and k_2), are also related to Gibbs energies as before if entropy contributions can be neglected, the rate constants can be obtained from the activation energy ΔE^\ddagger , according to the Arrhenius equation.

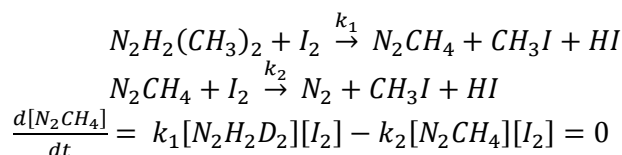
$$k_{\text{rxn}} \approx \left(\frac{K_B T}{h} \right) \left[\exp \left(-\Delta G^\ddagger / RT \right) \right]$$

Here K_B and h are the Boltzmann and plank constants, respectively, at room temperature and for ΔE^\ddagger in atomic unit (au), k_{rxn} is given by;

$$k_1 = 6.2 \times 10^{12} [\exp(-1060G_1^\ddagger)], \quad k_2 = 6.2 \times 10^{12} [\exp(-1060G_2^\ddagger)]$$

Kinetic parameters	
Activation energies	$\Delta E_1^\ddagger = -200.32 \text{ kJ/mol}$ $\Delta E_2^\ddagger = 18.93 \text{ kJ/mol}$
Equilibrium constant	$K_{\text{eq}} = 1.096$
Reaction rate constants	$k_1 = 6.722 \times 10^{12} \text{ sec}^{-1}$ $k_2 = 6.1528 \times 10^{12} \text{ sec}^{-1}$

The rate law derivation



i.e. applying steady state approximation;

$$\begin{aligned}
 &k_1[N_2H_2(CH_3)_2][I_2] = k_2[N_2CH_4][I_2] \\
 &[N_2CH_4] = \frac{k_1[N_2H_2(CH_3)_2][I_2]}{k_2[I_2]} = \frac{-k_1[N_2H_2(CH_3)_2]}{k_2}
 \end{aligned}$$

Substitute the value of $[N_2CH_4]$ into;

$$\begin{aligned}
 \text{Rate} &= \frac{d[P]}{dt} = -k_2[N_2CH_4][I_2] \\
 \text{Rate} &= k_2 \left(\frac{k_1[N_2H_2(CH_3)_2]}{k_2} \right) [I_2] \\
 \text{Rate} &= k_1[N_2H_2(CH_3)_2][I_2]
 \end{aligned}$$

The reaction is second order.

As the time which this report was written there were no published materials on the mechanism of the reaction of 1,1-dimethylhydrazine with iodine. Geometrical optimization of intermediate, transition

states, reactants and products in the reaction of 1,1-dimethylhydrazine with iodine was done using DFT and semi-empirical method (MNDO), the electronic energy and the heat of formation determined were shown in tables above.

The plausible mechanism for the oxidation of 1,1-dimethylhydrazine by iodine is shown as;

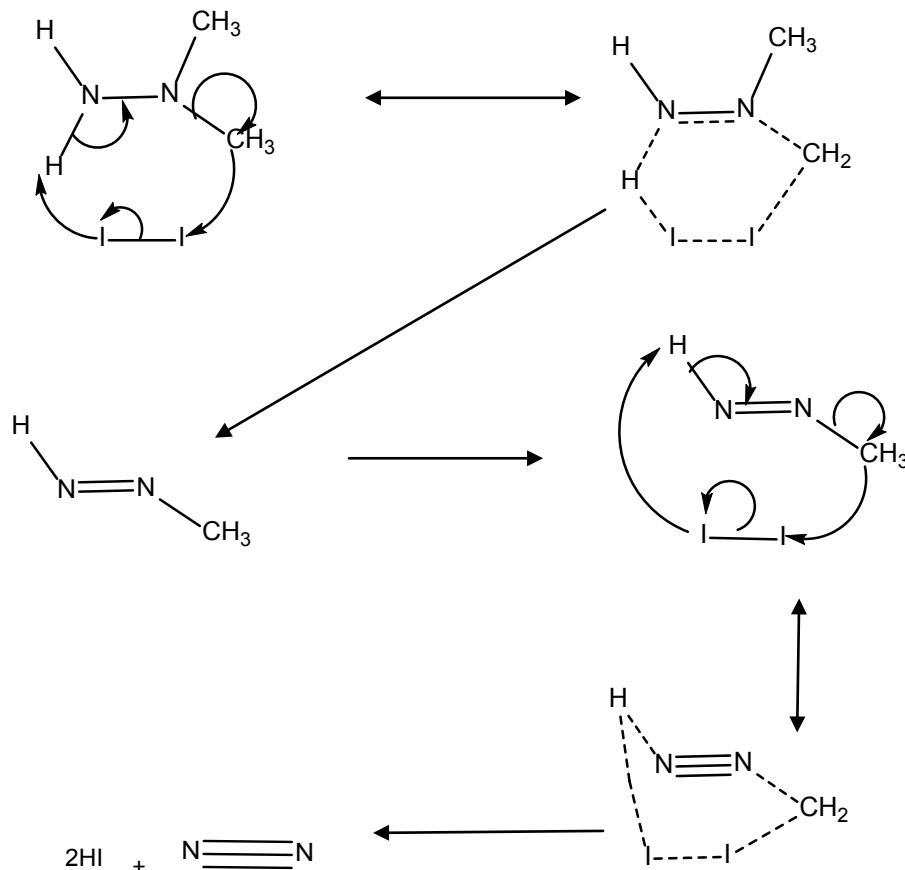


Figure 2 Reaction scheme for the proposed mechanism.

The scheme above can be represented in a simplified two step form as;



So that the overall equation for the reaction is given by Eq. (3); i.e.



The symbol D from the rate law derivation step represents CH_3 , In step 1: the optimized 1,1-dimethylhydrazine reacted with iodine molecule and produced 1-methyldiazene, hydrogeniodide and methyl iodide via TS1, while in step 2: 1-methyldihydrazene which was found to be a highly reactive (as confirmed from the binding energy) of the molecule, its optimized structure reacted with another iodine molecule to yield another hydrogen iodide molecule, methyl iodide and nitrogen gas. The summation of Eqs. (1) and (2) above gave Eq. (3), which is the proposed stoichiometric equation for the oxidation of 1,1-dimethylhydrazine by iodine.

The energy profile diagram (**Figure 1**) depicts the two step mechanism of the oxidation of 1,1-dimethylhydrazine by iodine based on DFT calculations, with the positions of the various species. From the diagram it was evident that step 1 is the rate determining step as shown by the high position of the transition state, TS1. IR analysis confirmed that TS1 and TS2 were actually the transition states in each step.

The enthalpy of reaction was computed using the stoichiometric equation (Eq. (3)) and it was estimated to be -2.53 kJmol^{-1} , indicating that the reaction is exothermic and as such a little heat is released into the environment [16]. The energies of activation were computed by DFT and were estimated to be 18.93 and -200.32 KJ/mol . From the result the free energy of activation was computed for step 1 and 2 using DFT, while the rate constant k_1 and k_2 were also estimated to be 6.722×10^{12} and $6.1528 \times 10^{12} \text{ sec}^{-1}$, respectively. This result shows that step 1 is the slowest and rate determining step as depicted by the smaller value of k_2 compared to k_1 [17].

Conclusions

In the reaction the activation energy was found to be negative in the first step, while its positive in the second step (under DFT calculations) indicating that the second step could easily decompose to form back the reacting species or if the temperature is reduced so as to reduce the excess activating energy of the reactants then the formed transition state can proceed through the forward reaction to form the proposed products. The kinetics would then have to be reconstructed into 2 processes, one in the presence of a steady room temperature and the other for a drop in the temperature required for the second step to proceed to completion. From this research it is highly unlikely that the second step would proceed on an uncontrolled environment or without the aid of a catalyst, since the intermediate N_2CH_4 is not stable as seen from its binding energy.

References

- [1] U.S. Environmental Protection Agency. Health and environmental effect profiles for 1,1-dimethylhydrazine. EPA/600/x-84/134. *Environmental Criteria and Assessment Office*. Office of Research and Development, Cincinnati, 1984.
- [2] Agency for Toxic substances and diseases registry (ATSDR). Toxicological profile for hydrazine's, public health service, US Department of Health and Human Services, Atlanta, GA, 1997.
- [3] DC Young. *Semi-Empirical Methods in Computational Chemistry: A Practical Guide for Applying Techniques to Real World Problems*. John Wiley and Sons, New York, 2002.
- [4] U.S. Department of Health and Human Services. *Registry of Toxic Effects of Chemical Substances (RTECS, online database)*. National Toxicology Information Program, National Library of Medicine, Bethesda, MD, 1993.
- [5] JE Amooore and E Hautala. Odor as an aid to chemical safety: Odor thresholds compared with threshold limit values and volatilities for 214 industrial chemicals in air and water dilution. *J. Appl. Toxicol.* 1983; **3**, 272-90.
- [6] GD Clayton and FE Clayton. *Patty's Industrial Hygiene and Toxicology*. Vol XI. John Wiley and Sons, New York, 1981.
- [7] The Merck Index. *An Encyclopedia of Chemicals, Drugs and Biological*. 11th ed. EDS Buda Van, Merck and Co., Railway, New Jersey, 1989.

- [8] U.S. Department of Health and Human Services. *Hazardous Substances Databank (HSDB, online database)*. National Toxicology Information Program, National Library of Medicine, Bethesda, 1993.
- [9] S Globig and KJ Freundt. Metabolism of hydrazobenzene in rat liver homogenate. *Naunyn-Schmiedeberg's Arch. Pharmacol.* 1996; **354**, R28.
- [10] M Onoue, S Kado, Y Sakaitani, K Uchida and M Morotomi. Specific species of intestinal bacteria influence the induction of aberrant crypt foci by 1,2-dimethylhydrazine in rats. *Cancer Lett.* 1997; **113**, 179-86.
- [11] GA Shallangwa, A Uzairu, VO Ajibola and H Abba. MNDO and DFT computational study on the mechanism of the oxidation of 1,2-diphenylhydrazine by iodine. *Phys. Chem.* 2014; **2014**, 592850.
- [12] K Ayub and T Mahmood. DFT studies of halogen bonding abilities of nitrobenzene with halogens and chlorofluorocarbons. *J. Chem. Soc. Pakistan* 2013; **35**, 617-821.
- [13] Spartan Users Guide, version 3.0. Wavefunction, 1993.
- [14] A Mondal and R Banerjee. Kinetics and mechanism of uncatalyzed oxidation of hydrazine with superoxide coordinated to cobalt(III). *Indian J. Chem. A* 2009; **48**, 645-9.
- [15] P Bhatnagar, RK Mittal and YK Gupta. Stoichiometry, kinetics, and mechanism of the oxidation of hyponitrous acid by iodine in acetate buffers. *J. Chem. Soc. Dalton Trans.* 1990, 3669-73.
- [16] T Engel and P Reid. *Physical Chemistry*. Pearson Prentice Hall, Upper Saddle River, New Jersey, USA, 2006.
- [17] RP Szajewski and GM Whitesides. Rate constants and equilibrium constants for thiol-disulfide interchange reactions involving oxidized Glutathione. *J. Am. Chem. Soc.* 1980; **102**, 2011-26.